

Article

An Example-Guide for Rapid Seismic Assessment and FRP Strengthening of Substandard RC Buildings

Sousana Tastani ^{1,*} and Georgia Thermou ^{2,*} ¹ Civil Engineering Department, Democritus University of Thrace, 671 00 Xanthi, Greece² Civil Engineering Department, The University of Nottingham, Nottingham NG7 2RD, UK

* Correspondence: stastani@civil.duth.gr (S.T.); georgia.thermou@nottingham.ac.uk (G.T.)

Abstract: This paper presents a rapid seismic assessment and Fibre Reinforced Polymer (FRP) retrofit design methodology which relies on the European design guidelines recently published in Chapter 8 of fib Bulletin 90 on the use of externally applied FRP reinforcement in the seismic retrofitting of reinforced concrete (r.c.) structures. For this purpose, an example-guide is developed with step-by-step hand calculations aiming to facilitate engineers of practice and researchers working in the field to easily understand the proposed methodology. A three-storey, pilotis-type residential r.c. building is selected typical of the Mediterranean construction practice in the 1970s. The methodology followed only aims to provide preliminary results on seismic assessment and retrofitting before the implementation of more sophisticated analysis if need be (e.g., in case of irregular buildings). The assessment procedure identified that the columns of the ground storey, being the most critical structural elements for the stability of the structure, are vulnerable to brittle failure modes. To remove all the brittle failure modes attributed to inherent deficiencies and enhance the overall deformation capacity of the building, the strengthening schemes applied in the ground storey (pilotis) is a combination of local strengthening measures, such as FRP wrapping, and global interventions. The latter may refer to the addition of r.c. jacketing to the central column to remove slenderness and of metal X-braces to modify the lateral deflection shape of the building and thus moderate the interstorey displacement demand.

Keywords: assessment; buildings; concrete; substandard r.c. detailing; global and local interventions; FRP jacketing



Citation: Tastani, S.; Thermou, G. An Example-Guide for Rapid Seismic Assessment and FRP Strengthening of Substandard RC Buildings. *Appl. Sci.* **2022**, *12*, 12950.

<https://doi.org/10.3390/app122412950>

Academic Editor:
Giuseppe Lacidogna

Received: 9 November 2022

Accepted: 12 December 2022

Published: 16 December 2022

Publisher's Note: MDPI stays neutral with regard to jurisdictional claims in published maps and institutional affiliations.



Copyright: © 2022 by the authors. Licensee MDPI, Basel, Switzerland. This article is an open access article distributed under the terms and conditions of the Creative Commons Attribution (CC BY) license (<https://creativecommons.org/licenses/by/4.0/>).

1. Introduction

In Europe, the use of externally applied FRPs in retrofitting of r.c. structures has been a subject of continuous research since the 1990s with numerous published papers, reports and successful research projects. The technical Bulletin on Externally bonded FRP reinforcement for r.c. structures ([1], and references therein) by the fib (International Federation of Concrete) Task Group 9.3 summarized the knowledge at that time and provided detailed design guidelines on the use of FRP, the practical execution and the quality control, based on the expertise and state-of-the-art knowledge of the task group members back in 2001. Its main purpose was to cover most of the design problems rather than tackling in detail all the aspects of r.c. strengthening with FRP composites. The first applications in construction appeared the same period, e.g., in Greece after the 1999 Athens earthquake, as a pressing need for immediate enhancement of the seismically vulnerable old structures (the problem of the seismic vulnerability of the existing building stock refers to methods to predict possible effects at the occurrence of seismic events and to develop prioritization plans for risk mitigation, see, i.e., [2,3]: a prioritization plan could include, i.e., FRP retrofitting). Since then, a significant amount of progress has been made that is reflected in the new Task Group 5.1 Bulletin 90 [4]. Especially Chapter 8, also presented in [5], summarizes design guidelines which are based on the comparative assessment of

past models, requirements established from first principles and reference is made to the available experimental data ([6–25] and references therein). Alternative retrofit strategies for the seismic strengthening with composite materials are presented considering the overall response of the existing structure. Apart from detailing of FRP interventions for seismic applications, in addition global interventions need to be considered provided that on first assessment it is deemed necessary to also moderate the deformation demand by increasing the effective stiffness of the structure. This approach is common in existing r.c. buildings where system deficiencies in lateral stiffness distribution along the height of the building (e.g., soft stories) are combined with lightly reinforced concrete members that possess limited deformation capacity [26,27].

The novelty of the methodology [4,5] lies in the use of performance-based design criteria for the assessment and retrofitting at both local and global level of existing structures. Based on the concepts developed, damage is expected to occur when the displacement demand imposed by the seismic excitation exceeds the displacement capacity of the individual members. The use of FRP jacketing at local level (i.e., structural element level) aims to modify the hierarchy of strengths by suppressing any premature failure mode (i.e., shear, anchorage/splice, compression reinforcement buckling) that usually occurs in old-type r.c. structural members due to improper seismic detailing and promote flexural failure. The addition of FRP jacketing at existing r.c. structural members with inherent deficiencies, however, does not affect the flexural strength, and thus the translational stiffness of the structures. Therefore, when enhancement of translational stiffness is deemed necessary, global retrofit measures should be applied.

The objective of this paper is to deliver an example-guide based on hand calculations of an existing multi-story r.c. building, representative of the older construction practice, which is going to be strengthened with the use of FRPs following the conceptual framework developed in Chapter 8 of Bulletin 90 [4,5]. The example-guide provides a step-by-step overview of the response of the building at local and global level and decisions on whether global strengthening measures need to be adopted along with measures at local level using FRPs. Furthermore, it sheds light to the detailed calculations entailed to perform assessment and design of the retrofit schemes. The ambition is that the example guide will provide a useful reference to the engineers of practice, researchers working in the field, university educators and students, and thus help in the wider application of the methodologies proposed in [4,5].

2. Synopsis of the Methodology

The methodology [4,5] comprises two stages; assessment and retrofitting at both local and global structural level. The assessment starts upon knowledge of the building's geometry, materials properties, and reinforcing detailing of the primary elements (columns, beams). The axial loads of the ground floor columns are calculated based on the seismic combination and the elements' slenderness is checked. Those columns subjected to high axial loads are considered susceptible to brittle failure, thus rendering them critical for the stability of the structure. The deformation capacity (in terms of drift at yielding and at ultimate) and flexural strength are assessed. The methodology suggests alternative approaches to estimate the deformation capacity aiming to demonstrate the easiness in application of each approach and the differences in the yielding values. At this stage the secant to yield translational stiffness is estimated and the effective period of the structure is calculated and directly related to demand in terms of elastic spectral displacement. The deformation capacity of the existing members is dictated by the type of deficiency identified and needs to be modified accordingly (i.e., in case of insufficient shear strength, short lap splices).

Strengthening at global level aims to modify the lateral response shape of the building by controlling the distribution of interstorey drift height-wise. This is achieved by the addition of stiffness along the height of the building as to comply with the target period value (lower than the effective period and closer to the code requirement) and the target

response shape (i.e., target interstorey drift distribution). Design charts are used to facilitate the procedure of defining the required increase in stiffness per storey. In general, an exceedance of the code's reference period value no higher than 25% and a shear-type shape leads to reduced intervention cost. The seismic displacement demand is recalculated for the strengthened building and demand at structural element level is defined. Based on the assessment outcome and if the ductility capacity is below demand, then the required FRP number of plies need to be calculated. In case of columns, the addition of FRP reinforcement also aims to alleviate brittle modes of failure (i.e., shear, lap-splice, compression bar buckling). Special attention is attributed to the external, beam-column joints which are not laterally supported by transverse beams and do not have sufficient detailing (i.e., horizontal stirrups).

3. Assessment

3.1. Description of the Building: Materials and Detailing

The 3-storey residential r.c. frame building has a plan $10\text{ m} \times 12\text{ m}$ (Figure 1a) and total height $H_{\text{tot}} = 9\text{ m}$. The storey height is 3 m , the clear column height is $H = 2.7\text{ m}$, and thus the shear span length is $L_V = H/2 = 1.35\text{ m}$. Only the upper two storeys have masonry infills, whereas the ground storey is open (pilotis type of building, Figure 1b).

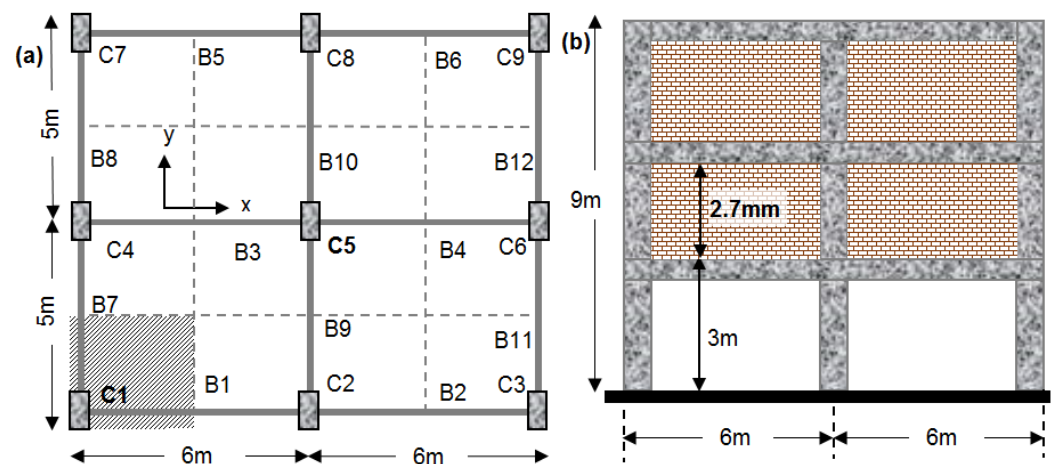


Figure 1. (a) Plan view of a typical storey and (b) elevation view of the building.

Typical columns have a rectangular cross section with $h = 350\text{ mm}$ and $b = 250\text{ mm}$, reinforced internally with six longitudinal bars of diameter $D_b = 14\text{ mm}$, with clear cover $c = 20\text{ mm}$ and effective depth d about the strong axis x being $d = 350 - 20 - 0.5 \times 20 = 323\text{ mm}$. The reinforcing ratio is $\rho_l = A_s/bh = 1.06\%$. The columns' transverse reinforcement comprises stirrups of $D_{b,st} = 6\text{ mm}$ at 150 mm centres, all anchored with 90° hooks at the ends (Figure 2a); this shear reinforcement is of poor effectiveness both due to its magnitude and anchorage detailing. The lap splicing length is developed at the bottom of the column and consists of a straight part $l_o = 50 D_b = 700\text{ mm}$ with end hook (Figure 2a). In this case, the effective splice length is artificially increased by $12.5 D_b$ aiming to account for the influence of the hook (thus $l_o = 62.5 D_b = 875\text{ mm}$). All beams have a cross section height of $h = 400\text{ mm}$ (including the flange thickness that is equal to the slab thickness, $h_{\text{slab}} = 200\text{ mm}$) and breadth $b = 200\text{ mm}$, reinforced as presented in Figure 2b. The beam transverse reinforcement comprises stirrups of $D_{b,st} = 6\text{ mm}$ at 250 mm centres anchored with 90° hooks at the ends. The materials mean strength is considered for the assessment procedure [28]: the mean in situ cylindrical concrete compressive strength is $f_{cm} = 16\text{ MPa}$ (by following [29]). The longitudinal reinforcement is ribbed steel StIV with an average yield strength based on tests of extracted samples $f_{ys} = 500\text{ MPa}$. Transverse reinforcement is smooth steel StI with an average yield strength based on tests of extracted samples $f_{yw} = 240\text{ MPa}$.

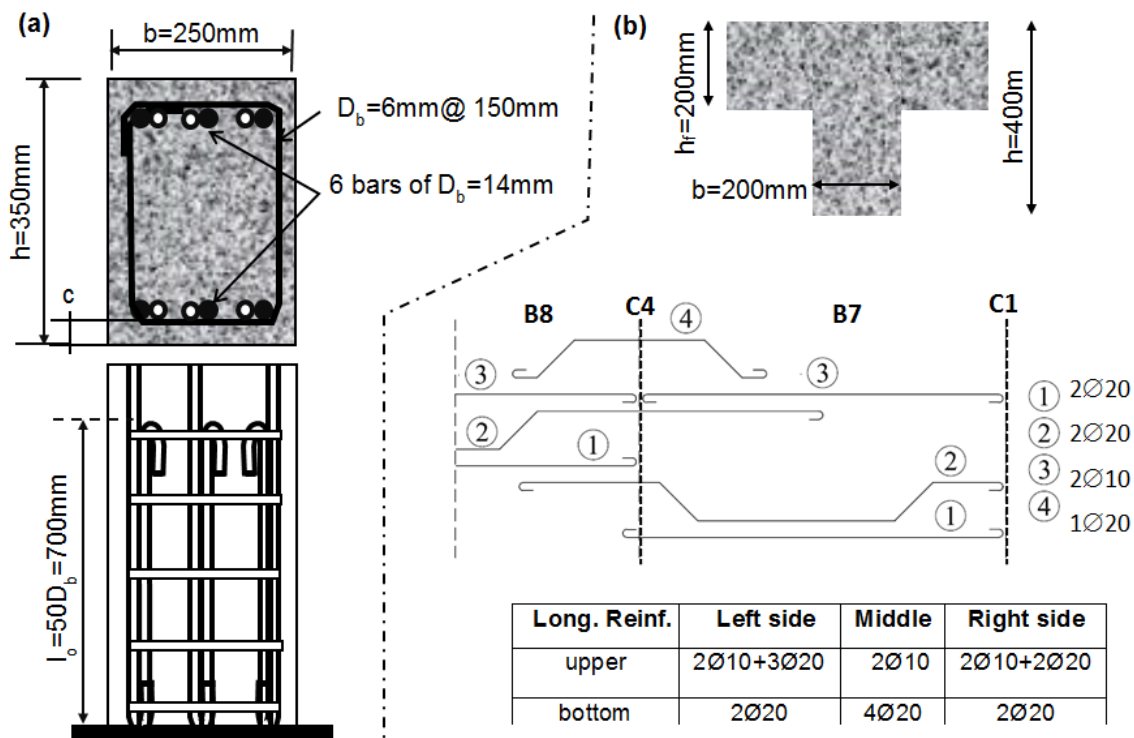


Figure 2. (a) Column cross section detailing and splice arrangement at column base and (b) beam geometry and longitudinal reinforcement detailing.

3.2. Assessment of Pilotis Columns

In a pilotis-type frame structure (i.e., common practice in Greece and southern countries in Europe) infill walls are absent in the ground storey bays to allow for parking or shop windows. The lateral deformation imposed by the seismic loading localizes in the ground floor due to the low stiffness compared to that of the upper floors, thus acting as a soft storey. Therefore, an assessment of ground floor columns is critical since earthquake events have revealed that ground columns' failure precedes that of beams (for beams a similar assessment procedure may be followed, not presented here due to page limitations).

3.2.1. Slenderness

A first step is to check the slenderness of the columns. The total gravity load of each floor, W_{floor} , is calculated by the seismic combination, $G + 0.3 Q$, where G stands for the total dead load (25 kN/m^3 of reinforced concrete for the slab of thickness $h_f = 0.2 \text{ m}$ and additional 2 kN/m^2) and Q is the total live load (3.5 kN/m^2), hence, $W_{\text{floor}} = \text{plan area} \cdot (Gh_f + 0.3 Q) = 120 \text{ m}^2 \cdot (25 \times 0.2 + 2 + 0.3 \times 3.5) = 966 \text{ kN}$ whereas the total weight carried by the building's ground floor columns is $W_{\text{tot}} = 3 \times 966 = 2900 \text{ kN}$ (three floors). For simplicity the weight of the external brick masonry walls of the 2nd and 3rd floor was not considered in the building mass because it represents about 5–10% of the weight of the r.c. elements. For example, the masonry weight per floor is $W_{\text{masonry}} \approx 165 \text{ kN}$ (see the detailed calculation in Table A1 of Appendix A—the same is valid for the next calculations where it is deemed necessary). Thus, the total masonry weight is 330 kN—this is an upper limit since the calculation does not consider any openings. Each ground column undertakes part of the total axial load after multiplying W_{tot} by the ratio of the tributary area (i.e., the light hatched area as per column C1 in Figure 1a) to the total floor area. The values of axial loads N_{Ed} along with the corresponding axial load ratios, $v_{\text{Ed}} = N_{\text{Ed}} / (bhf_{\text{cm}})$ are $N_{\text{Ed}} = 181.3 \text{ kN}$ — $v_{\text{Ed}} = 0.13$ for the corner columns C1/3/7/9, and $N_{\text{Ed}} = 362.5 \text{ kN}$ — $v_{\text{Ed}} = 0.26$ for all the peripheral columns C2/4/6/8. The central column C5, by having $N_{\text{Ed}} = 725 \text{ kN}$ — $v_{\text{Ed}} = 0.52$, is prone to crushing before yielding due to the high

axial load. In order to reduce v_{Ed} below 0.4, thus securing a dominant flexural response, the increase in the cross-section dimensions is required. The slenderness effect is taken into consideration by following the procedure of ACI 318-19 [30]. The radius of gyration for the cross section of the column with respect to the weak axis y-y (Figure 1a) is $i = \sqrt{I_g/A_g} \approx 0.3 b = 75 \text{ mm}$ and the associated slenderness is $\lambda = (\beta_o \cdot H)/i = 36 > \lambda_{lim} = \max\{25; 15/\sqrt{v_{Ed}} = 20.8\} = 25$. The reduction in slenderness is achieved by increasing the cross section to $h^{new} = 450 \text{ mm}$ and $b^{new} = 350 \text{ mm}$. The new calculations are: $v_{Ed}^{new} = 0.29$, $i^{new} \approx 0.3 b^{new} = 105 \text{ mm}$ and $\lambda^{new} = 25.7 < \lambda_{lim} = \max\{25; 27.9\} = 27.9$. Note that $v_{Ed}^{new} = 0.29$ is an upper value given that the increase in the cross section dimensions is usually implemented by using concrete of higher quality.

3.2.2. Deformation and Strength Indices from Flexure

The strength and deformation capacity were assessed as per the response of the building in y-y direction (strong axis: bending about x-x in Figure 1a). The corner columns are expected to yield first due to the lower axial load. The central column C5 is susceptible to crushing before yielding due to the high axial load. For lightly reinforced concrete elements, the curvature at the onset of tension reinforcement yielding ϕ_y is approximated $\phi_y = (2\varepsilon_{sy})/h = 2 \times 0.0025/350 = 0.0143/\text{m}$, common for all columns. The moment at yielding as per the point of action of the concrete force can be approximated by Equation (1):

$$M_y = A_{s1} \cdot f_{ym} \cdot jd + N_{Ed}(0.5 h - 0.4 \times 0.25 \cdot d) \tag{1}$$

where $jd = 0.85 d$ is the internal lever arm between tensile force of bottom steel reinforcement and concrete compressive force and $A_{s1} = 3 \times \pi \times 14^2/4 = 462 \text{ mm}^2$ is the area of tensile reinforcement. The implementation of Equation (1) for corner columns ($N_{Ed} = 181.3 \text{ kN}$) results to $M_y \approx 89 \text{ kNm}$ and for peripheral columns ($N_{Ed} = 362.5 \text{ kN}$) to $M_y \approx 115 \text{ kNm}$. A more precise calculation of curvature and moment at yielding can be deduced from cross section analysis by using Response2000 [31], where for corner columns $\phi_y = 0.0128/\text{m}$, $M_y = 90 \text{ kNm}$ and for peripheral columns $\phi_y = 0.0148/\text{m}$, $M_y = 109 \text{ kNm}$. The two procedures for definition of ϕ_y , M_y result to similar values.

The curvature at ultimate $\phi_u = \varepsilon_{cu}/(\xi d)$, at concrete crushing strain $\varepsilon_{cu} = 0.0035$, may be found by using the graph of Figure 3 (similar graphs were derived in [32]): for symmetrically reinforced cross section (present case), the normalized compression zone $\xi = x/d$ ($d = 323 \text{ mm}$) is plotted against the total longitudinal reinforcing ratio ρ_l for several axial load ratios. This graph was deduced at yielding of tensile reinforcement; aiming to address the fact that at ultimate the compressive zone x becomes shorter, a reduction factor 0.9 is also applied to ξ value. Thus, for $\rho_l = 1.06\%$ for corner columns ($v_{Ed} = 0.13$) is $\xi = 0.24$ and $\phi_u = 0.0035/(0.9 \times 0.24 \times 323) = 0.05/\text{m}$ and for peripheral ($v_{Ed} = 0.26$) is $\xi = 0.27$ and $\phi_u = 0.044/\text{m}$. All useful values of the assessment are summarized in Table 1.

Table 1. Results from cross section analysis and rotation capacity.

Cross Section Analysis: Approximations					Chord Rotation from Procedures (a–c)				
Column	$\phi_y = 2\varepsilon_{sy}/h$ (1/m)	M_y (kNm)	K (kNm ⁻¹)	ϕ_u (1/m) – ξ from Figure 3	θ_y (%)	(a): θ_u (%) ($\mu_\theta = \theta_u/\theta_y$)		(b): θ_u (%) ($\mu_\theta = \theta_u/\theta_y$)	(c): θ_u (%) ($\mu_\theta = \theta_u/\theta_y$)
						$I_{pl} = 160 \text{ mm}$	$I_{pl} = 615 \text{ mm}$		
1/3/7/9 $v_{Ed} = 0.13$	0.0143	89	3810	0.05–0.24	0.64	0.8 (1.2)	1.6 (2.4)	2 (3.1)	1.7 (2.7)
2/4/6/8 $v_{Ed} = 0.26$						0.73 (1.1)	1.4 (2.2)	1.7 (2.6)	1.8 (2.8)

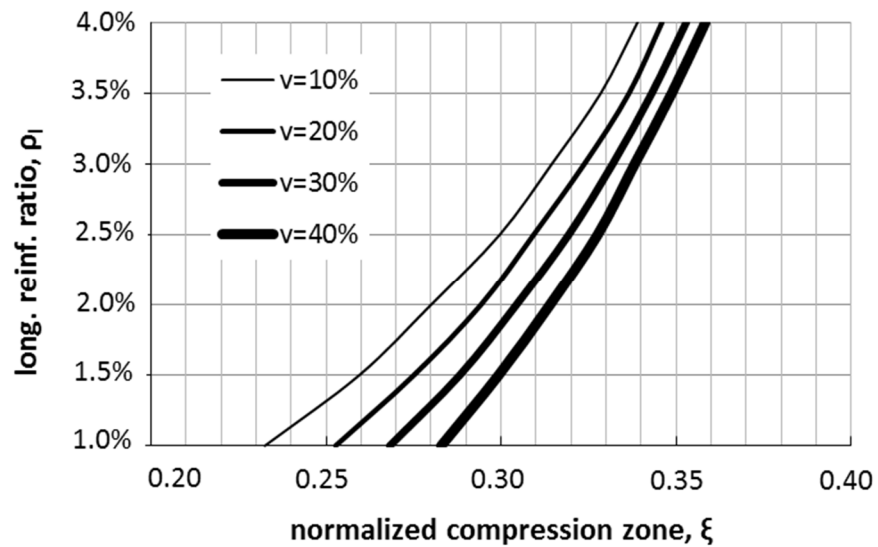


Figure 3. Estimation of compression zone depth at ultimate for symmetrically reinforced concrete cross section with variables being the axial load and the amount of reinforcement.

The secant to yield effective stiffness of the columns is given as $EI = M_y / \phi_y$. Hence, for the two groups of columns: (i) $EI = 89 / 0.0143 \approx 6250 \text{ kNm}^2$ for corner columns, (ii) $EI = 115 / 0.0143 \approx 8050 \text{ kNm}^2$ for peripheral one. For concrete grade C16/20 the Young Modulus is $E = 29 \text{ GPa}$, the moment of inertia of uncracked section is $I = bh^3 / 12 = 8.93 \times 10^8 \text{ mm}^4$ (no consideration of internal reinforcement) thus the elastic stiffness is $EI_{el} \approx 25,900 \text{ kNm}^2$. This is near threefold the effective values above (in pushover analysis cross sections are assumed cracked, hence 50% of the elastic value is used, $EI_{cr} = 50\%EI_{el} = 12,950 \text{ kNm}^2$). The secant to yield translational stiffness of the columns is calculated by using $K = 12 EI / H^3$. For corner columns $K = 12 \times 6250 / 2.7^3 = 3810 \text{ kNm}^{-1}$ and for peripheral columns $K \approx 4910 \text{ kNm}^{-1}$ whereas the elastic and that of the cracked cross section values are $15,790 \text{ kNm}^{-1}$ and 7895 kNm^{-1} , respectively. By comparing values of K , the order of magnitude of the error for the estimated translational stiffness may be large, depending on the adopted approach. This difference has a great impact on the structure period of vibration, and thus on the maximum displacement that is going to be developed during the earthquake. Later, in Section 4, the secant to yield translation stiffness is used in defining the effective translational period T_{eff} of the building (Table 1).

The chord rotation at yielding is approximated as $\theta_y = (\phi_y H) / 6 = (0.0143 \times 2.7) / 6 = 0.64\%$. A more detailed expression of this property is [33]:

$$\theta_y = 1/3\phi_y(a_v z + L_V) + 0.0014(1 + 1.5 h / L_V) + 0.125\phi_y D_b f_{sy} / \sqrt{f_{cm}} \tag{2}$$

with $a_v z = 0$ (it is assumed that shear cracking is not expected to precede flexural yielding), $L_V = 1350 \text{ mm}$ (i.e., half the column clear height), $h = 350 \text{ mm}$, $D_b = 14 \text{ mm}$, $f_{sy} = 500 \text{ MPa}$ and $f_{cm} = 16 \text{ MPa}$. Equation (2) results to $\theta_y = 1.15\%$ that is almost double of the simplified estimation ($\theta_y = 0.64\%$). However, the most conservative value $\theta_y = 0.64\%$ is used in the following calculations because it is testified in relevant tests on substandard columns as a lower bound magnitude [34].

The ultimate chord rotation θ_u is estimated by following the three alternative procedures presented in chapter 8 of [4] and are summarized in Table 1. More specifically:

- (a) From basic mechanics:

$$\theta_u = 1 / \gamma_{el} [\theta_y + (\phi_u - \phi_y) l_{pl} (1 - 0.5 l_{pl} / L_V)] \tag{3}$$

where γ_{el} is equal to 1.5 for primary members, $\theta_y = 0.64\%$, ϕ_u is the ultimate curvature of the end section evaluated by assigning the concrete ultimate strain $\epsilon_{cu} = 0.0035$ (values are shown in Table 1). The plastic hinge length l_{pl} can be estimated from three alternatives, as:

$$l_{pl} = 0.1 L_V + 0.17 h + 0.24 (D_b f_{sy}) / \sqrt{f_{cm}} \tag{3a}$$

$$l_{pl} = 0.2 h [1 + 1/3 \min (9, L_V/h)] \tag{3b}$$

$$l_{pl} = 0.5 d \tag{3c}$$

Their implementation results to $l_{pl(3a)} = 615$ mm or $l_{pl(3b)} = 160$ mm or $l_{pl(3c)} = 161.5$ mm, respectively. Note that Equation (3b) considers cyclic loading and Equation (3c) is a simple definition of l_{pl} for members with old type detailing. The results of Equation (3b,c) coincide. The difference in results for l_{pl} obtained from Equation (3a–c) is considerably high and affects the estimations of the elements' ductility. For example, for corner columns $\theta_u(l_{pl} = 615 \text{ mm}) = 1.6\%$ or $\theta_u(l_{pl} = 160 \text{ mm}) = 0.8\%$. The corresponding rotation ductility is $\mu_\theta = \theta_u/\theta_y = 1.6/0.64 = 2.4$ or $\mu_\theta = 0.8/0.64 = 1.2$. Apparently, the results in Table 1 for $l_{pl} = 160$ mm suggest that all columns—except of the middle one—fail close to yielding demonstrating no ductility. For $l_{pl} = 615$ mm all columns demonstrate adequate ductility in the order of 2.

(b) Empirically, by following the proposed Equation (4a,b):

$$\mu_\phi = 0.45 \epsilon_{cu,c} / (\epsilon_{sy} \nu_{Ed}) \text{ for } \nu_{Ed} \geq 0.2 \text{ and } \mu_\phi = 0.45 \epsilon_{cu,c} / \epsilon_{sy} \times h / \xi d \text{ for } \nu_{Ed} < 0.2 \tag{4a}$$

$$\mu_\theta = \theta_u / \theta_y = \mu_\Delta = 0.5(\mu_\phi + 1) \tag{4b}$$

where, term ξ from Table 1 should be multiplied with 0.9 (as previously explained), $\epsilon_{cu,c} = 0.0035$, $\epsilon_{sy} = 0.0025$ and $\theta_y = \phi_y H / 6 = \epsilon_{sy} (H/h) / 3 = 0.64\%$. The μ_θ value shall be multiplied by 1.5 to account for the contribution of reinforcement pullout to the rotation capacity. Implementing Equation (4a,b) for example for columns C1/3/7/9 ($\nu_{Ed} = 0.13 < 0.2$), result in $\mu_\phi = 3.16$ and $\mu_\theta = 1.5 \times [0.5 \times (3.16 + 1)] = 3.1$ and $\theta_u = 3.1 \cdot 0.64\% = 2\%$. This value of θ_u [Table 1, column denoted as (b)] is close to that calculated above in procedure (a) when using $l_{pl} = 615$ mm from Equation (3a).

(c) The value of the plastic part of the chord rotation capacity of concrete members under cyclic loading is given by the following calibrated Equation (5) (from [33]):

$$\theta_u^{pl} = \frac{1}{\gamma_{el}} 0.0185 \times 0.48 \left(1 + \frac{\alpha_{sl}}{1.6}\right) (0.25)^\nu \left[\frac{\max(0.01, \omega')}{\max(0.01, \omega)}\right]^{0.3} f_c^{0.2} \left(\frac{L_V}{h}\right)^{0.35} \times 25^{\left[\frac{\alpha_w \rho_{wy} f_{yw}}{f_c}\right]} 1.275^{100\rho_d} \tag{5}$$

where $\theta_u = \theta_y + \theta_u^{pl}$ ($\theta_y = 0.64\%$). The implementation of this expression is demonstrated for corner columns C1/3/7/9: $\gamma_{el} = 1.8$, $\alpha_{sl} = 1$ because slippage of vertical bars from their anchorage or lap-splice at the lower end of the column is physically possible (presence of splices), $\nu = 0.13$, $\omega = \rho_{s1} f_{sy} / f_c = 0.53\% \times 500 / 16 = 0.165$, and ω' (even if $\rho_{s1} = \rho_{s2} = 0.5\rho_l = 0.53\%$) is taken double of ω due to the presence of splices, $f_c = 16$ MPa, $f_{sy} = 500$ MPa, $L_V = 1350$ mm, $h = 350$ mm, $\rho_d = 0$ (absence of diagonal reinforcement), $\rho_{wy} = A_{sy} / (s_n b) = 2 \times (\pi \times 6^2 / 4) / (150 \times 250) = 0.15\%$ (ratio of transverse steel parallel to the direction of loading, here y-direction), $\alpha_w = 0.14$ (confinement effectiveness factor, limited contribution because stirrups are sparse) and $f_{yw} = 240$ MPa. This results in $\theta_u^{pl} = 2.33\%$ and $\theta_u = 0.64\% + 2.33\% \approx 3\%$. For the peripheral columns the calculations lead to $\theta_u = 0.64\% + 1.95\% = 3.1\%$. It is important to note that in this procedure (c) the presence of splice l_o in the vicinity of plastic hinge length deteriorates the plastic rotation when

$l_o < l_{ou,min}$ and then the total rotation capacity should be multiplied by $l_o/l_{ou,min}$; term $l_{ou,min}$ is given by Equation (5a,b):

$$l_{ou,min} = \frac{D_b f_{sy}}{\left[\left(1.05 + 14.5 a_1 \rho_{wy} f_{yw} / f_c \right) \sqrt{f_c} \right]} \quad (5a)$$

$$a_1 = (1 - s_h / (2b_o)) \times (1 - s_h / (2h_o)) \times n_{restr} / n_{tot} \quad (5b)$$

Their implementation results to $a_1 = 0.32$ and $l_{ou,min} = 1513$ m. The hooked splice may be assumed as sufficient detailing for earthquake resistance (no need to divide with 1.2). Because $l_o = 875$ mm $< l_{ou,min} = 1513$ mm, thus the ultimate rotation for the corner columns is $\theta_u = 875/1513 \times 3\% = 1.7\%$ and for peripheral columns, $\theta_u = 875/1513 \times 3.1\% = 1.8\%$.

The calculations of θ_u deduced by the three procedures (a–c), led to μ_θ results higher than 2, however when considering a narrow plastic length, they may receive values close to 1. The demonstration of the three procedures aims at highlighting the easiness or complexity each one encompasses as per its implementation.

3.2.3. Brittle Mechanisms: Shear and Lap-Splices

The calculations in Section 3.2.2 for determining the flexural response of the ground storey columns ignored the columns' shear capacity. The preceding calculations are meaningful provided the columns are able to develop the lateral force V_{fl} that corresponds to flexural capacity, i.e., $V_{fl} = M_y / L_V$. Thus, for corner columns $V_{fl} = 89/1.35 \approx 66$ kN and for peripheral $V_{fl} = 115/1.35 \approx 85$ kN. Note that V_{fl} should be multiplied by a safety factor >1 aiming to account for the over-strength of columns. More specifically, in accordance with EN1998-1 [35], for medium ductility r.c. buildings (DCM), the over-strength for beams and columns may be found by the product of the flexural capacity with (i) the material safety factor 1.15 for steel, (ii) a factor equal to 1.2 due to design-action effects at the end sections of critical regions, and (iii) a factor equal to 1 and 1.1 due to steel strain hardening for beams and columns, respectively. Thus, for columns the overstrength factor is $1.15 \times 1.2 \times 1.1 \approx 1.5$. The shear capacity of the columns is given by Equation (6) (from [33]):

$$V_{Rd,o} = 1/\gamma_{el} \{ (h - x)/(2L_V) \cdot \min(N, 0.55A_c f_c) + [1 - 0.05 \min(5, \mu_\theta^{pl})] (V_{Rd,c} + V_{Rd,s}) \} \quad (6a)$$

$$V_{Rd,c} = 0.41 \sqrt{f_c} b \times x \quad (6b)$$

$$V_{Rd,s} = \rho_{sw,y} b_o h_o f_{y,st} = A_{sy} / (s_h b_o) b_o h_o f_{y,st} \quad (6c)$$

where $\gamma_{el} = 1.15$, $x = \xi d$ (ξ from Table 1, multiplied also with the correction factor 0.9 as explained before). Applying Equation (6b,c), for corner columns result to $V_{Rd,c} \approx 29$ kN, for peripheral to $V_{Rd,c} \approx 32$ kN and $V_{Rd,s} = 28$ kN. For the definition of $\mu_\theta^{pl} = (\theta_u - \theta_y) / \theta_y = \mu_\theta - 1$, among procedures (a–c) above, procedure (b) is chosen because it results to a more conservative estimation of $V_{Rd,o}$. Thus for the corner columns the term $[1 - 0.05 \min(5, \mu_\theta^{pl})]$ in Equation (6a) is $[1 - 0.05 \min(5, 3.1 - 1)] = 0.89$ and for peripheral columns is 0.92 ($\mu_\theta^{pl} = 2.6 - 1 = 1.6$). Next, Equation (6a) is implemented: for corner columns is $V_{Rd,o} \approx 60$ kN $< 1.5 V_{fl} = 1.5 \times 66 = 99$ kN and for peripheral $V_{Rd,o} = 80$ kN $< 1.5 V_{fl} = 1.5 \times 85 \approx 128$ kN.

It may conclude that both corner and peripheral columns will fail in shear near yielding at almost the same drift ($\theta_y V_{Rd,o} / V_{fl}$: for corner columns is $0.64\% \times 60/66 = 0.59\%$ and for peripheral $0.64\% \times 80/85 = 0.6\%$).

Another concern is whether the available splice length l_o suffices for the reinforcing bars to develop their yielding strength. The available bond strength is given by Equation (7):

$$\tau_b = 2\mu_{fr} / (\pi D_b) \times [2c f_{ctk} + 0.33 (A_{st} f_{y,st}) / (N_b s)] \quad (7)$$

and yielding is secured when $\tau_b \geq \gamma_{el} D_b f_{sy} / (4l_o)$. Values for the parameters are: $\mu_{fr} = 1$, $D_b = 14$ mm, $f_{ctk} = 0.33 f_{cm}^{0.5} = 0.33 \times 16^{0.5} = 1.3$ MPa, $c = 20$ mm, $A_{st} = 2 \times \pi \times 6^2 / 4 = 56.5$ mm², $f_{y,st} = 240$ MPa, $N_b = 3$ bar pairs, $s = 150$ mm, $\gamma_{el} = 1.15$, $f_{sy} = 500$ MPa, thus

Equation (7) yields to $\tau_b = 2.82$ MPa. For a splice with a hook ($l_o = 875$ mm) is $\tau_b = 2.8$ MPa $>$ $\gamma_{el} D_b f_{sy} / (4l_o) = 2.3$ MPa, thus lap splice suffices longitudinal reinforcement yielding, but after that milestone (where $\mu_\theta > 1$) cover cracking is anticipated; this implication diminishes cover contribution (i.e., $2c_{fctk} \approx 0$) in defining bond strength thus a splice failure is also anticipated.

From the preceding assessment analysis, it may be concluded that the ground columns may suffer shear failure before any yielding of the longitudinal reinforcement that occurs at a drift of 0.6%; the latter corresponds to lateral displacement at the top of the ground storey $\Delta = 0.6\% \times 2.7$ m = 16 mm. [Note: If a straight splice without hook detailing was used, then lap splice failure is also anticipated for both the peripheral and the corner columns before yielding].

4. Global Strengthening Requirements

The strengthening of the existing building should consider whether the available effective stiffness, K_{eff} , suffices to resist the seismic demand or if there is need to moderate, i.e., the drift demand. In the latter case, the retrofit solution should include global intervention measures to increase K_{eff} along with local interventions like FRP jacketing for alleviating brittle modes of failure (Figure 4a). Note that by increasing K_{eff} the demand may be reduced in two different ways: (a) a higher effective stiffness results in a lower predominant period tending towards the left in the displacement spectrum, and (b) through a more uniform distribution of deformation demand in the structure, which secures that the magnitude of deformation demanded by individual members is lowered.

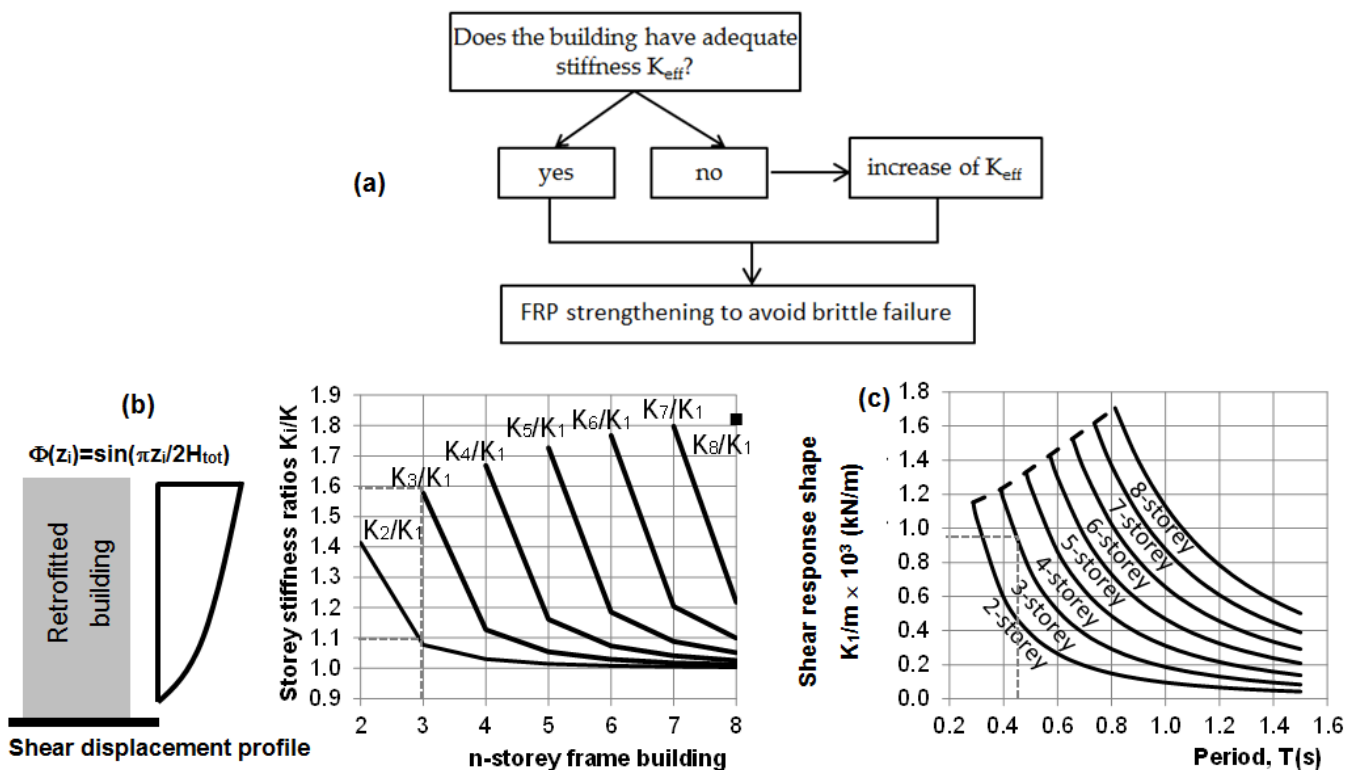


Figure 4. (a) Flowchart on the decision of implementing local and/or global interventions. For shear deflection shape (b) Storey stiffness ratios k_i ($= K_i/K_1$) and (c) corresponding stiffness to mass ratio for the first storey, K_1/m_1 , versus period (note to obtain required K_1 values multiply the ordinate by the mass m , in tons).

The necessary calculations for global measures are based on Appendix 8.2 of [4]. More specifically, the total building mass is $M = 290$ tonnes. The effective translational period T_{eff} is calculated based on the secant to yield sectional analysis for the definition of individual

column translational stiffness K . By assuming that the building has a soft first storey (i.e., pilotis-type), then practically all lateral translation is concentrated in the ground storey ($K_{eff} = \sum_{i=1}^n K_i \Delta\Phi_i^2 = K_1 \times 1^2 = K_1$). Thus, the translational stiffness against seismic sway of the ground storey is (direction y-y): $K_{eff} \approx 38,690$ kN/m. Note that column's C5 stiffness was taken conservatively as the least among the other two groups. Its reinforcement does not reach yielding due to the applied high axial load. Therefore, the effective period is $T_{eff} = 2\pi\sqrt{(M/K_{eff})} = 2 \times 3.14 \times \sqrt{(290/38,690)} = 0.54$ s. The empirical reference value T_{ref} in EN 1998-1 [35] is $T_{ref} = 0.075 H_{tot}^{3/4} = 0.075 \times 9^{3/4} = 0.39$ s. Because $T_{eff}/T_{ref} = 0.54/0.39 = 1.4$, T_{eff} exceeds by more than 25% the empirical T_{ref} . Thus, K_{eff} should be increased to lower T_{eff} to an acceptable range of values, i.e., 0.4–0.45 s for a three-storey building.

The target or improved period, T_{trg} , of the retrofitted structure may be selected based on experience, as a value between T_{ref} and the initial T_{eff} . A note of caution is that the cost of the intervention increases as T_{trg} is reduced getting closer to T_{ref} . Besides, an increase in K_{eff} is required aiming at modifying the lateral deflection shape (fundamental response shape) due to localization of deformation at the ground floor columns (i.e., the assumed in Figure 5b). For the seismic assessment of the building, the peak ground acceleration was considered $PGA = 0.24$ g and the soil class as B. For $T_{eff} = 0.54$ s, the elastic spectral displacement demand is estimated from Equation (8) for $T_C \leq T \leq T_D$ (from [35]):

$$S_d(T) = a_g S \eta \beta_o (T_C T) / 40 \tag{8}$$

where $S = 1.2$ (soil class B), $T_C = 0.5$ s, $T_D = 2$ s, $a_g = 0.24$ g, $\eta = 1$ ($\xi = 5\%$) and $\beta_o = 2.5$, hence $S_d = 0.048$ m. The elastic displacement S_d will induce a lateral drift in the pilotis $\theta = S_d/H = 0.048/2.7 \approx 1.8\%$ which corresponds to drift or displacement ductility demand of $\mu_\theta = \mu_\Delta = 1.8/0.64 = 2.8$. According to Table 1, and after the implementation of only local measures to alleviate the brittle shear failure, the drift supply by considering the most conservative procedure a is lower than the demand for all columns. The reduction in the drift demand along with the improvement of the deflection shape of the pilotis-type building requires the increase in pilotis stiffness (i.e., adoption global intervention measures) before any application of FRP jacketing (local measures).

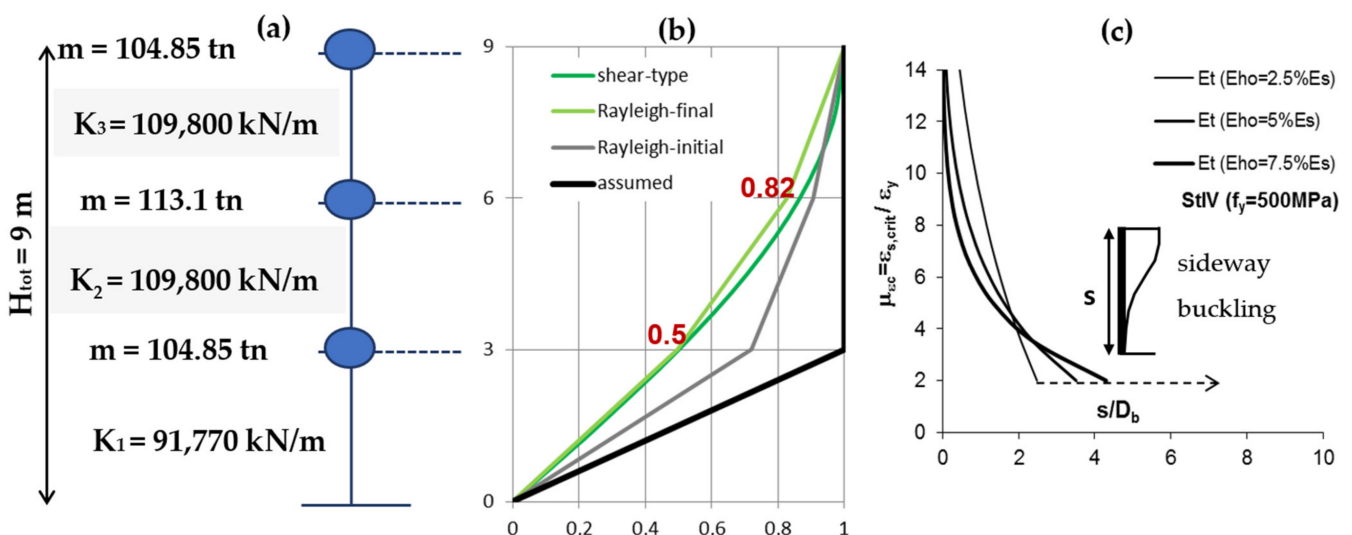


Figure 5. (a) Stiffness distribution of the enhanced building and (b) its lateral displacement profile after performing Rayleigh iterative method. (c) Compressive strain ductility μ_{ec} versus stirrup spacing s/D_b for StIV.

The selection of a shear-type drift distribution along the building's height (Figure 5b) reduces the required intervention because a soft storey formation may be re-engineered towards this option for moderate improvement. By using the charts of Figure 4b,c result in the following target values for the storey stiffness ratios K_i/K_1 : $K_2/K_1 = 1.1$ and

$K_3/K_1 = 1.6$ (see the dashed lines in Figure 4b, K_1 stands for the ground floor or first floor). For the chosen target period $T_{trg} = 0.45$ s and by using Figure 4c, the required ground storey stiffness is $K_1/m_1 = 950$ kN/m, which once multiplied with storey mass $m_1 = 96.6$ tn results in $K_1 = 91,770$ kN/m, also, $K_2 = 1.1 \times 91,770 \approx 100,950$ kN/m and $K_3 = 1.6 \times 91,770 \approx 146,830$ kN/m for the 2nd and 3rd floor, respectively. The target stiffness value of the ground storey, $K_1 = 91,770$ kN/m, is much larger than the available $K_{eff} = 38,690$ kN/m. Such a stiffness increase in ground storey may be achieved partly by the need to increase the central column cross section due to slenderness effect and by adding metallic cross bracings in the direction of the seismic action under consideration (here the direction is y-y).

The central column of increased cross section (350×450 mm) is assumed as being pinned at the base with elastic stiffness $K_{C5,new} = 3EI/H^3 = 11,748$ kN/m (the initial value was 3810 kN/m). The required cross braces stiffness is deduced as: $\Sigma K_\chi = K_1 - K_{C5,new} - 4$ corner columns $\times 3810$ kN/m $- 4$ peripheral columns $\times 4910$ kN/m $\approx 45,140$ kN/m. The span of each brace is $L = 5$ m $- 1.5 \times 0.35$ m $= 4.475$ m and $\phi = \arctan(h_{st,cl}/L) = 0.6$ thus $\phi = 31^\circ$ ($h_{st,cl} = 2.7$ m). The length of the brace diagonals is $D = \sqrt{(4475^2 + 2700^2)} = 5226$ mm. The stiffness of braces is (modulus of elasticity for cast steel sections, $E_s = 150,000$ MPa): $\Sigma K_\chi = 45,140$ kN/m $= 2E_s A_{br}/D \cos^2 \phi = 2 \times 150,000 \times A_{br}/5226 \times \cos^2(31^\circ)$ thus $A_{br} \approx 1100$ mm². By adding two braces symmetrically (i.e., by connecting columns C1–C4 and C6–C9), then each brace should have total cross section $A_{br} = 650$ mm².

After the increase in the pilotis stiffness under the requirement of a shear-type deflection shape using the charts of Figure 4b, one could validate this simple solution by performing the Rayleigh iterative method and considering the stiffness of the exterior infill walls of the upper floors. More specifically, in each of the upper two floors, for two exterior solid walls in y-y direction of a total cross section area $A_w = 2 \times (10$ m $- 3 \times 0.35$ m) $\times 0.12$ m ≈ 2.15 m² or $\rho_{mw} = A_w/(A_{floor} = 120$ m²) ≈ 0.018 and for $h_i = 2.7$ m, $f_{bc} = 5$ MPa, $f_{mc} = 5$ MPa (each is divided by $\gamma_m = 1.5$), and $\mu_y^{mw} = 2.5$, $\theta_y^{mw} = 0.15\%$, then the masonry wall stiffness in each floor is: $K_{mw} \approx A_{floor}/h_i \times (0.1f_{bc}^{0.7} f_{mc}^{0.3})/(\mu_y^{mw} \theta_y^{mw}) \times \rho_{mw,i} \approx 71,100$ kN/m. The available effective stiffness of the 2nd and 3rd floor are then: $K_2 = K_3 = K_{eff} + K_{mw} = 38,690 + 71,100 \approx 109,800$ kN/m (Figure 5a). Because the available magnitudes K_2 and K_3 are higher than or close to the required for the chosen shear-type response of the building (i.e., $K_2 = 100,950$ kN/m and $K_3 = 146,830$ kN/m), there is no need for global measures in these floors. For the Rayleigh iterative method, the floor mass (i.e., 96.6 tonnes) is increased by adding a share of the total masonry weight $W_{masonry} = 33$ tonnes; thus $W_{masonry}$ was distributed as $\frac{1}{4}$ in each of the ground and the 3rd floor and $\frac{1}{2}$ in the 2nd floor. After such analysis, the deflection shape presented in Figure 5b was obtained (the light green coloured curve titled Rayleigh-final) and is very close to the shear-type on which the addition of stiffness was based. Moreover, from this analysis the calculated period is found 0.46 s, very close to the target value $T_{trg} = 0.45$ s. In addition, the initially assumed lateral deflection shape and the initial approximated shape by using the Rayleigh method are plotted in Figure 5b for comparison reasons (the masonry mass and stiffness of the upper floors is considered).

For the selected period $T_{trg} = 0.45$ s ($< T_C = 0.5$ s), the elastic spectral displacement demand is estimated from Equation (9) (from [35]):

$$S_d(T) = a_g S \eta \beta_o T^2 / 40 \quad (9)$$

where $a_g = 0.24$ g, $S = 1.2$ (soil class B), $\eta = 1$ ($\xi = 5\%$) and $\beta_o = 2.5$, thus $S_d = 0.036$ m. Considering that this displacement will be increased by about 20% when transferring from the spectrum (Equivalent Single Degree of Freedom) to the actual structure (Multi-Degree of Freedom), then, the relative drift demand at the ground storey ($\Delta\Phi = 0.5$, Figure 5b) is $\theta_{dem} = 1.2 \times 0.5 \times S_d/H = 0.8\%$, which corresponds to a ductility demand of $\mu_\theta = \mu_\Delta = 0.80\%/0.64\% = 1.25$. This demand is very close to the supply when a short plastic hinge length is considered [procedure (a) in Table 1]. To improve ductility and to alleviate premature shear failure, FRP jacketing is required.

5. Local Strengthening through FRP Jacketing

The objective is to remove, through FRP jacketing, brittle failure modes so that the flexural capacity of columns can be fully developed. The design methodology adopted follows the procedure described in Chapter 8 of [4,5]. FRP confinement is applied as to enhance (i) displacement ductility, (ii) shear strength, and additionally, to prevent failure due (iii) buckling of steel longitudinal bars. For the needs of the current example, a generic carbon FRP fabric with the following mechanical properties was selected for column and beam retrofiting: thickness $t_o = 0.12$ mm, modulus of elasticity: $E_f = 165,000$ MPa, ultimate tensile stress: $f_{fu} = 2970$ MPa and ultimate strain $\varepsilon_{fuk} = 0.018$. The design tensile strain $\varepsilon_{fu,h}$ in the FRP layer shall not exceed the limit: $\varepsilon_{fu,h} = \eta_1 \cdot \eta_2 \cdot \eta_3 \cdot \varepsilon_{fuk} / \gamma_f$ where $\gamma_f = 1.5$ for fully wrapped FRP arrangement (i.e., the ground floor RC frames do not accommodate any masonry). Factors η_1, η_2, η_3 are considered as follows:

- Factor η_1 accounts for the radius of chamfer $R (= c + 0.5D_b = 20 + 7 = 27$ mm), at the corners of the member: $\eta_1 = 0.25 + 2(2R + D_b)/h' = 0.25 + 2(2 \times 27 + 14)/(350 - 2 \times 27) = 0.71 < 1$ (h' is the straight part of the largest cross section side).
- Factor $\eta_2 = 1$ accounts for the sufficiency of the wrap development length: the straight parts of the cross section sides $h' \approx 300$ mm and $b' \approx 200$ mm suffice to accommodate the minimum anchorage length of the external FRP layer $l_b^{\min} = 0.5\pi\sqrt{(E_f \times t_o \times s_o / \tau_a)} = 0.5\pi\sqrt{(165,000 \times 0.12 \times 0.5/5)} \approx 70$ mm (s_o and τ_a are slip and bond strength values, provided by the resin manufacturer); to this end the external layer of the FRP jacket can be anchored over the column's shorter side.
- Factor $\eta_3 = 1$ for fully wrapped jacket (considers the redundancy of the jacket against debonding).

Accordingly, the design tensile strain $\varepsilon_{fu,h}$ in the FRP layer is $\varepsilon_{fu,h} = \eta_1 \cdot \eta_2 \cdot \eta_3 \cdot \varepsilon_{fuk} = 0.71 \times 1 \times 1 \times 0.018/1.5 = 0.0085$.

Given the required displacement ductility ($\mu_\phi = 1.25$) from Section 4, the associated curvature ductility is $\mu_\phi = 2\mu_\theta - 1 = 2 \times 1.25 - 1 = 1.5$. The maximum compression strain demand is $\varepsilon_{cu,c} = 2.2\mu_\phi \varepsilon_{sy} \nu_{Ed}$ [from Equation (4a)]. For the corner columns ($\nu_{Ed} = 0.13$) $\varepsilon_{cu,c} = 2.2 \times 1.5 \times 0.0025 \times 0.13 = 0.0011 < 0.0035$ and for the peripheral columns ($\nu_{Ed} = 0.26$) $\varepsilon_{cu,c} = 0.0021 < 0.0035$. From these calculations, it is concluded that there is no need for confinement of concrete through closed FRP jackets to meet its strain demands in the compression zone resulting from the displacement ductility calculation.

According to Section 3, flexural response dominates when the shear strength V_{Rd} exceeds $1.5 V_{fl}$. For the simplicity of the following calculations it is taken as $1.5 V_{fl} = \max(1.5 V_{fl,corner}, 1.5 V_{fl,peripheral}) \approx 128$ kN and also the available $V_{Rd,o} = \min(V_{Rd,o,corner}, V_{Rd,o,peripheral}) = 60$ kN. The difference $\Delta V = 1.5 V_{fl} - V_{Rd,o} = 68$ kN will be resisted by FRP closed-type jacketing as $\Delta V = V_{Rd,f} = (2t_f/b) \times bh \times E_f \times \varepsilon_{fu,h}$, which it results to $t_f = 0.07$ mm $< t_o = 0.12$ mm. A single layer suffices for shear strengthening along the column's height.

For the lap-splices, even if the available bond strength $\tau_b = 2.82$ MPa [from Equation (7)] due to cover and stirrups contributions suffices for bar yielding [$\tau_b = 2.82$ MPa $> \gamma_{el} D_b f_{sy} / (4l_o) = 2.3$ MPa], however it is reduced after that milestone because cover is cracked [term $2cf_{ctk}$ in Equation (7) is set equal to 0]. The contribution of FRP jacketing in restoring the bond strength to the yielding limit is given by Equation (10):

$$\tau_b = 2\mu_{fr} / (\pi D_b) [0.33 A_{st} f_{y,st} / (N_b \cdot s) + 2t_f E_f \varepsilon_{f,sl} / N_b] \quad (10)$$

thus, for $D_b = 14$ mm, $\mu_{fr} = 1$, $N_b = 3$, $\varepsilon_{f,sl} = 0.0015$, $t_f = nt_o$, $A_{st} = 2 \times \pi \times 6^2/4 = 56.5$ mm², $f_{y,st} = 240$ MPa and $s = 150$ mm Equation (10) results to $t_f = 0.25 = nt_o = n \times 0.12$, or $n = 2$ layers needed to wrap the splice region of $l_o = 700$ mm, that is developed at the bottom of the column.

To eliminate potential buckling of compressive bars, given the required curvature ductility, $\mu_\phi = 1.5$, the compression strain demand is $\varepsilon_{cu,c} < 0.0035$ for both the corner and the peripheral columns (as previously was checked from $\varepsilon_{cu,c} = 2.2\mu_\phi \varepsilon_{sy} \nu_{Ed}$). From

the buckling curve of Figure 5c (case StIV- $f_y = 500$ MPa and sideway buckling) and for $s/D_b = 150/14 \approx 11$, the strain at which the bar will become unstable is $\mu_{\epsilon_c} \approx 2 = \epsilon_{s,crit} / \epsilon_{s,y}$ thus $\epsilon_{s,crit} = 2 \times 0.0025 = 0.005$. Hence, for the estimation of the required jacket confinement, it must be ensured that $\epsilon_{cu,c} \geq \max(\epsilon_{cu,c} = 0.0035, \epsilon_{s,crit} = 0.005) = 0.005$. Equation (11a–c) correlate term $\epsilon_{cu,c}$ with the FRP jacketing:

$$\epsilon_{cu,c} = \epsilon_{cu} + 0.075[\zeta \times (\alpha_f \rho_{fv} E_f \epsilon_{fu,h} + \alpha_w \rho_{sv} f_{y,st}) / f_c - 0.1] \geq \epsilon_{cu} \tag{11a}$$

$$\alpha_f \approx 1 - ((b - 2R)^2 + (h - 2R)^2) / (3bh) \tag{11b}$$

$$\rho_{fv} = 2t_f(h + b) / (hb) \tag{11c}$$

with $\epsilon_{cu} = 0.0035$, $\zeta = 1$ (for $\epsilon_{cu,c} \leq 0.01$), $\alpha_f = 0.56$, $\alpha_w = 0.15$, $\rho_{sv} = 0.00314$ and $\epsilon_{fu,h} = 0.0085$ (as previously calculated); thus Equation (11a) results to $\rho_{fv} = 0.0023$ and $\rho_{fv} = 2t_f(b + h) / (bh)$, which in turn corresponds to $n = 2$ layers along the critical regions of all columns, top and bottom, of length $l_{p1} = 615$ mm (for simplicity of the intervention this length is rounded to 600 mm).

Given the above calculations for elimination of premature buckling and splice failure, the applied jacketing (2 layers result to $t_f = 0.24$ mm and thus to $\rho_{fv} = 0.0033$) offers a limited displacement ductility. This is testified through Equation (12):

$$\mu_{\Delta} = 1.3 + 12.4 \times (0.5 \times \alpha_f \rho_{fv} E_f \epsilon_{fu,h} / f_c - 0.1) \geq 1.3 \tag{12}$$

Its implementation results to $\mu_{\Delta} = 1.06 \geq 1.3$ thus $\mu_{\Delta} = 1.3$. This supply suffices against the required value (as previously calculated $\mu_{\Delta} = 1.25$).

The FRP strengthening of the ground storey columns (except C5) is summarized as follows: a single CFRP layer is wrapped along the height of each column to alleviate shear failure, one additional CFRP layer is wrapped at the lower 700 mm of each column to strengthen the splice region, one additional CFRP layer is wrapped at the upper 600 mm of each column to alleviate compressive bar buckling (Figure 6a). Column C5 does not require any FRP intervention because the increase in its cross-section size is implemented through reinforced concrete jacketing. (Note: For beams, by following similar procedure, FRP U-shaped jacketing of two-layer strips of width 100 mm and spacing 100 mm along the element full length is required along with special details in the ends in order to secure the jacket against debonding, e.g., adhesive anchors, see Chapter 6 in [4], Figure 6a).

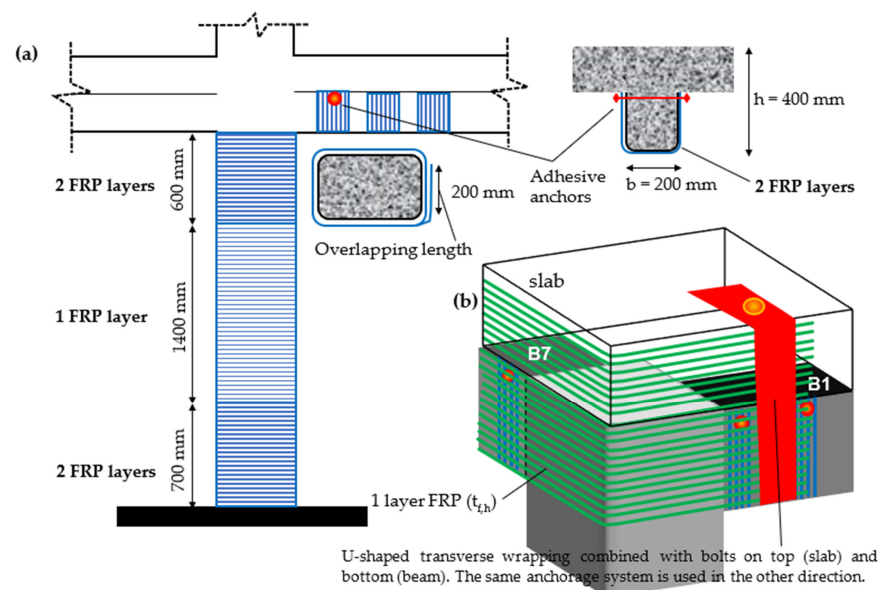


Figure 6. (a) FRP jacketing in ground floor columns and beam. (b) Strengthening of corner joint B1-C1-B7.

Beam-Column Joint Strengthening

External beam-column joints are not laterally supported on four sides by beams, hence require horizontal shear reinforcement to prevent deterioration due to cracking induced by the high shear stress demand. This demand is the result of the steep moment gradients as they facilitate reversal of moment from one face of the member to the other. In old structures, r.c. beam-column joints rarely had in their body horizontal stirrups. So, it is deemed necessary to retrofit such a critical element of the structure.

As it is observed in the plan layout of Figure 1a, T- and L-shaped (knee or corner) joints exist. The strengthening design procedure is presented in detail for the L-shaped joint B1-C1-B7 of the ground storey; apparently all other L-shaped joints of the ground floor follow the same requirements. It is noted that in Chapter 8 of fib Bulletin 90 [4] two design approaches are presented. In this example, Approach 1 is implemented aiming to determine the required amount of horizontal FRP reinforcement through its function as added shear reinforcement in the joint panel. Approach 1 generally leads to significant amount of FRP reinforcement because, in the interest of conservatism, neglects any confining contribution, which could in turn lead to a retrofit inferior to expectations.

The first step is to calculate the sums of yield moments in the beams and in the columns framing into the joint. Hence, ΣM_{yb} is the sum of yield moments of the beams that frame into the joint and ΣM_{yc} is the sum of yield moments of the columns that frame into the joint:

x-x direction—weak axis (C1–B1): Beam B1-left has yield moment 134 kNm. The yield moments of the column below and above the joint are 53 kNm ($N_{Ed} = 181.3$ kN) and 48 kNm ($N_{Ed} = 120.8$ kN), respectively (the cross-section analysis was performed using Response2000 [11]). Hence, $\Sigma M_{yc} = 53 + 48 = 101$ kNm $< \Sigma M_{yb} = 134$ kNm. By being columns weaker than beams, they define the magnitude of shear stress in the joint. Hence, the vertical shear force $V_{j,v}$ is derived by following the Greek Code for Assessment and Retrofit [36], from Equation (13) as:

$$V_{j,v} = \Sigma M_{yc}(1/jd_c - 1/L_{b,n} \cdot H_n/H) + 1/2 |(V_{g+\psi q,b})_l - (V_{g+\psi q,b})_r| \quad (13)$$

where jd_c is the internal lever arm of the column section, H_n and H are the theoretical and clear storey heights, and $L_{b,n}$ is the theoretical half span of the beam. The beams are considered as fully fixed at their ends. The load from the slabs is assumed to be transferred to beam B1. Conservatively, it is assumed that the loads transferred from the slab to B1 correspond to a quarter of the area of the slab. Hence, the total linear load for the seismic combination is estimated as $g = 9.75$ kN/m, $q = 4.38$ kN/m and $g + 0.3q = 11.06$ kN/m, hence $(V_{g+\psi q,b})_l = (g + 0.3q)l/2 = 33.19$ kN. Then, by implementing Equation (13) results to $V_{j,v} = 510.8$ kN. The horizontal shear force $V_{j,h}$ acting in the joint is obtained from: $V_{j,h} = V_{j,v} \times h_c/h_b = 510.8 \times 250/400 = 319.2$ kN with upper limit of: $V_{j,h} \leq 80\% \times \eta f_{cm} \sqrt{(1 - v_{Ed}/\eta)} \cdot b_j h_{jc}$ where $\eta = 0.6(1 - f_{ck}/250) = 0.58$, $b_j = \min[\max(b_c, b_b), \min(b_c, b_b) + h_c/2] = 250$ mm and $h_{jc} = 250 - 2 \cdot d_2 = 250 - 2 \times 27 = 196$ mm. Thus $V_{j,h} = 319.2$ kN < 334.4 kN.

y-y direction—strong axis (C1–B7): The yield moment of beam B7-right is 134 kNm. The yield moments of the column below and above the joint are ~90 kNm and 83 kNm: $\Sigma M_{yc} = 83 + 90 = 173$ kNm $> \Sigma M_{yb} = 134$ kNm. By being beams weaker than columns, they define the magnitude of shear stress in the joint. The horizontal shear force $V_{j,h}$ is derived by following the Greek Code for Assessment and Retrofit [36], from Equation (14) as:

$$V_{j,h} = \Sigma M_{yb}(1/jd_b - 1/H_n \times L_{b,n}/L_b) \quad (14)$$

where $jd_b (=0.9 d; d = 370$ mm) is the internal lever arm of the beam section, H_n is the theoretical storey height, $L_{b,n}$ and L_b are the theoretical and clear half span of the beams, thus $V_{j,h} = 354.4$ kN with upper limit of $V_{j,h} \leq 80\% \cdot \eta f_{cm} \sqrt{(1 - v_{Ed}/\eta)} \times b_j h_{jc}$, $\eta = 0.6(1 - f_{ck}/250)$, where $b_j = 250$ mm, $\eta = 0.58$, $h_{jc} = 350 - 2 \cdot d_2 = 350 - 2 \times 27 = 296$ mm. Thus, $V_{j,h} = 354.4$ kN < 505 kN.

The horizontal shear force used for the calculation of the required FRP reinforcement, where fibers are oriented in the horizontal direction, is the maximum among 319.2 kN and 354.4 kN. For such a simple plan view of a building, one could deduce that the strong axis horizontal shear force apparently prevails. [Note: Alternatively, and with respect to the strong axis, the EN 1998-1 [35] for exterior beam-column joints proposes the simplified expression $V_{j,h} = 1.20A_{s1}f_y - V_{col}$, where A_{s1} is the top reinforcement of beam as $A_{s1} = 2 \times \pi \times 10^2/4 + 2 \times \pi \times 20^2/4 \approx 785 \text{ mm}^2$ (see Figure 2b) $f_y = 500 \text{ MPa}$ and V_{col} the shear force in the column above the joint as $V_{col} = M_y/L_V = 83/1.35 \approx 62 \text{ kN}$ hence $V_{j,h} \approx 410 \text{ kN}$, which should be lower than $80\% \cdot \eta f_{cm} \sqrt{(1 - v_{Ed}/\eta)} \cdot b_j h_{jc} = 505 \text{ kN}$. This approach increases the demand for FRP by almost 55 kN in comparison with what the most recent Code [36] deduces].

Prefabricated Carbon Fiber Reinforced Polymer (CFRP) plates will be used for the beam-column joint strengthening. An essential requirement is the proper anchorage of the FRP plates, otherwise FRP strengthening should not be considered effective. Fib Bulletin 90 [2] in its Section 9.2.3 provides details about anchorage of FRP strengthening in beam-column joints. The plates selected to be used have a thickness of $t_o = 1.4 \text{ mm}$, modulus of elasticity $E_f = 205,000 \text{ MPa}$, ultimate tensile stress $f_{fu} = 3200 \text{ MPa}$ and ultimate strain $\varepsilon_{fuk} = 0.017$. The design tensile strain ε_{fd} in the FRP layer shall not exceed the limit: $\varepsilon_{fd} = \varepsilon_{fuk}/\gamma_f = 0.017/3 = 0.0056$ where $\gamma_f = 3$ for FRP anchored on brittle substrate. According to fib Bulletin 90 [4] the allowable design value of FRP tensile strain shall not be taken higher than 0.004. Hence, $\varepsilon_{fd} = 0.004$. The thickness, $t_{f,h}$, is estimated from $t_{f,h} = \gamma_{Rd} \times V_{j,h}/(h_b \cdot E_f \cdot \varepsilon_{fd})$ as $t_{f,h} = 1.6 \text{ mm} > t_o = 1.4 \text{ mm}$. Because the calculated value is very close to t_o , given the increased conservatism the Approach 1 has, one layer of CFRP L-shaped plate is required by covering the full height of the beams (detailing as shown in Figure 6b).

6. Conclusions

The methodology [4,5] implemented for the development of the detailed example—guide uses performance-based design criteria for the assessment and retrofitting at both local and global level. Damage is identified when the displacement demand due to earthquake excitation exceeds the displacement capacity of the individual members. The addition of externally bonded FRP reinforcement aims to remedy any deficiencies in the response of existing structural members due to the lack of seismic detailing (i.e., sparse shear reinforcement, short anchorage/splices). Global measures are adopted to modify the lateral response shape of the building and control interstorey drift.

The conceptual framework [4,5] is applied to a case study of a pilotis-type multi-story r.c. building, representative of the older construction practice in Southern Europe in the '70s. The building is assessed and retrofitted using externally applied FRP jacketing. Hand calculations are provided which cover in detail all the steps required for assessment and retrofitting.

The implementation of the methodology, as it is outlined in Section 2, revealed the following: as per the assessment stage (i) the order of magnitude of the error for the translational stiffness when cracked cross section (7895 kNm^{-1}) or secant to yield (3810 kNm^{-1}) definition is adopted may be large; this difference (here 100%) has a great impact on the estimation of the structure's period of vibration, and thus on the maximum displacement reached during the seismic excitation; (ii) the estimated values of the deformation indices defined by using the alternative formulae included in [4,5] do not always agree with observations made on relevant experimental (the simplest formulae seem to estimate effectively the deformation indices); and (iii) the calculations of the deformation indices related to flexural response will not be realised when brittle failure modes are anticipated such as shear and lap splice which are repeatedly reported after a strong seismic event. At global level, interventions aim to lower the structure's period close to the code reference value and to re-design the lateral response shape of the building in response to a more uniform distribution of the interstorey drift. For local interventions FRP jacketing is applied. The FRP plies required are calculated firstly to suppress all possible premature modes of failure

(shear, bond, compression reinforcement buckling, exterior joints disintegration) and promote flexural response, and secondly to increase the ductility capacity in response to the seismic demand. Special attention needs to be given to the execution of the FRP application (i.e., corner rounding, special anchoring).

Author Contributions: Equal contribution by the two authors. All authors have read and agreed to the published version of the manuscript.

Funding: This research received no external funding.

Institutional Review Board Statement: Not applicable.

Informed Consent Statement: Not applicable.

Data Availability Statement: Not applicable.

Conflicts of Interest: The authors declare no conflict of interest.

Notation

A_g	gross area of concrete
A_s	total area of longitudinal steel reinforcement
D_b	diameter of longitudinal steel reinforcement
$D_{b,st}$	diameter of transverse steel reinforcement
E_c	modulus of elasticity of concrete
E_f	modulus of elasticity of FRP
E_s	modulus of elasticity of steel
H	clear height of column
H_{tot}	Height of building
K_j	translational stiffness of the column
L_v	shear span
N_{Ed}	Axial load of column
M_y	moment at yielding
M_{Rd}^o	the flexural strength
N_b	number of tensile splice pairs
L_{prov}	provided anchorage length of beam longitudinal reinforcement
R	radius of rounded corner
$T_{ref/eff/trg}$	reference, effective or target period
V_{Rd}	design shear resistance
$V_{Rd,c}$	the contribution of the concrete compression zone to the shear strength of the original member
$V_{Rd,f}$	shear strength of the FRP jacket
$V_{Rd,o}$	shear strength of the original member
$V_{Rd,s}$	the contribution of the web reinforcement to the shear strength of the original member
V_{fl}	lateral force at flexural strength ($=M_{Rd}^o/L_v$)
W_{tot}	total weight of the building due to the seismic combination $G + 0.3Q$
a_vz	the tension shift of the bending moment diagram
b	width of cross section (b' after chambering)
b_f	width of FRP strip
b_o	width of confined core in a column (to centerline of hoops)
c	the clear cover
d	effective depth of the member
f_c	concrete strength
f_{cm}	mean value of the concrete compressive strength
f_{ctk}	the concrete tensile strength
f_{fd}	design value of the FRP tensile strength
f_{ym}	mean value of the longitudinal steel yield strength, also referred as f_{sy}
f_{yw}	the mean yield strength of the shear reinforcement, also referred as $f_{y,st}$
h	total depth of the member (h' after chamfering)
h_{slab}	total depth of the slab

l_{pl}	plastic hinge length
l_o	splice length
i	radius of gyration for the cross section
n	the number of FRP layers placed in the jacket
n_l	the number of longitudinal reinforcing bars in the cross section
n_{floor}	the total number of floors of the building
s	spacing of hoops/stirrups
t_f	thickness of FRP
t_o	the thickness of a single layer
v_{Ed}	axial load ratio
x	depth of the compression zone
z	internal lever arm
ϕ_u	curvature at ultimate
ϕ_y	yield curvature
α	angle between fibres and the member axis perpendicular to the shear force
α_f	confinement effectiveness factor defined for FRP
α_w	confinement effectiveness factor defined for stirrups
γ_{el}	factor, greater than 1.00 for primary seismic members
γ_f	material safety factor for the FRP
$\varepsilon_{cu,c}$	the maximum compression strain demand
ε_{cu}	ultimate concrete strain
$\varepsilon_{fu,h}$	ultimate strain of the FRP jacket in the hoop direction
$\varepsilon_{s,crit}$	the strain at which the bar will become unstable
ε_{sy}	yield strain of the steel reinforcement
θ_u	ultimate chord rotation
θ_y	chord rotation at yielding
θ_u^{pl}	plastic part of the chord rotation capacity
μ_Δ	displacement ductility
μ_θ	chord rotation ductility
μ_ϕ	curvature ductility
$v_{d,max}$	the maximum axial load ratio
$\xi = x/d$	relative depth of the compression zone
ρ_s	longitudinal steel reinforcement ratio
ρ_{sw}	transverse steel reinforcement ratio
ρ_{fv}	the volumetric ratio of FRP reinforcement
ρ_{sv}	the volumetric ratio of transverse reinforcement
τ_b	bond strength

Appendix A

Table A1. Detailed computations of several assessment and retrofitting indices.

Formulae	Computation
masonry weight per floor: $W_{masonry} = \text{specific weight} \times \text{masonry thickness} \times \text{perimeter} \times \text{height}$	$W_{masonry} = 1200 \text{ Kgr/m}^3 \times 12 \text{ cm}$ (that is the total thickness of a two-layer bricks of breadth 6 cm) $\times 2 \times (9.95 + 11.25) \text{ m} \times 2.7 \text{ m} \approx 165 \text{ kN}$
slenderness effect: (i) the radius of gyration for the cross section of the column with respect to the weak axis y-y is $i = \sqrt{I_g/A_g} \approx 0.3b$ and (ii) the slenderness is $\lambda = (\beta_o \cdot H)/I$ and $\lambda < \lambda_{lim} = \max\{25; 15/\sqrt{v_{Ed}}\}$	Calculations for central column with $v_{Ed} = 0.52$: $i = \sqrt{I_g/A_g} \approx 0.3b = 0.3 \times 250 = 75 \text{ mm}$ $\lambda = (\beta_o \cdot H)/i = (1 \times 2700)/75 = 36$ and $\lambda = 36 > \lambda_{lim} = \max\{25; 15/\sqrt{0.52} = 20.8\} = 25$
Flexural strength: $M_y = A_{sl,1} \times f_{ym} \times jd + N_{Ed} \times (0.5 h - 0.4 \times 0.25 \cdot d)$	For corner columns ($N_{Ed} = 181.3 \text{ kN}$): $M_y = 462 \times 500 \times 0.85 \times 323 + 181.3 \times 10^3 \times (0.5 \times 350 - 0.4 \times 0.25 \times 323) \approx 89 \text{ kNm}$

Table A1. Cont.

Formulae	Computation
plastic hinge length l_{pl} (three alternatives): Equation (3a) Equation (3b) Equation (3c)	$l_{pl(3.a)} = 0.1 \times 1350 + 0.17 \times 350 + 0.24 \times (14 \times 500)/\sqrt{16} = 615 \text{ mm}$ $l_{pl(3.b)} = 0.2 \times 350 \times [1 + 1/3 \min(9, 1.35/0.35)] = 160 \text{ mm}$ $l_{pl(3.c)} = 0.5 \times 323 = 161.5 \text{ mm}$
ultimate chord rotation θ_u : $\theta_u = 1/\gamma_{el} [\theta_y + (\phi_u - \phi_y) l_{pl} (1 - 0.5 l_{pl}/L_V)]$	For corner columns: $\theta_u(l_{pl} = 615 \text{ mm}) = 1/1.5 \times [0.64\% + (0.05 - 0.0143) \times 0.615 \times (1 - 0.5 \times 0.615/1.35)] = 1.6\%$, or $\theta_u(l_{pl} = 160 \text{ mm}) = 1/1.5 \times [0.64\% + (0.05 - 0.0143) \times 0.16 \times (1 - 0.5 \times 0.16/1.35)] = 0.8\%$
Curvature ductility: Equation (4a) Equation (4b) μ_θ value shall be multiplied by 1.5 to account for the contribution of reinforcement pullout to the rotation capacity.	for corner columns ($\nu_{Ed} = 0.13 < 0.2$): $\mu_\phi = 0.45 \times 0.0035/0.0025 \times 350/(0.9 \times 0.24 \times 323) = 3.16$ and $\mu_\theta = 1.5 \times [0.5 \times (3.16 + 1)] = 3.1$ and $\theta_u = 3.1 \times 0.64\% = 2\%$
Equation (5b) Equation (5a)	$a_l = (1 - 150/(2 \times 210)) \cdot (1 - 150/(2 \times 310)) \times 4/6 = 0.32$ $l_{ou,min} = 14 \times 500/[1.05 + 14.5 \times 0.32 \times 0.00151 \times 240/16 \times \sqrt{16}] = 1513 \text{ m}$
Equation (6b) Equation (6c) Equation (6a)	for corner columns: $V_{Rd,c} = 0.41\sqrt{16} \times 250 \times 0.9 \times 0.24 \times 323/1000 \approx 29 \text{ kN}$ for peripheral: $V_{Rd,c} = 0.41\sqrt{16} \times 250 \times 0.9 \times 0.27 \times 323/1000 \approx 32 \text{ kN}$ $V_{Rd,s} = 2 \times (\pi \times 6^2/4)/(150 \times 210) \times 210 \times 310 \times 240/1000 = 28 \text{ kN}$ $V_{Rd,o} _{corner} = 1/1.15\{(350 - 0.9 \times 0.24 \times 323)/(2 \times 1350) \times \min(181.25, 0.55 \times 250 \times 350 \times 16/1000) + 0.89 \times (29 + 28)\} \approx 60 \text{ kN} < 1.5 V_{fl} = 1.5 \times 66 = 99 \text{ kN}$ $V_{Rd,o} _{periph.} = 1/1.15\{(350 - 0.9 \times 0.27 \times 323)/(2 \times 1350) \times \min(362.5, 0.55 \times 250 \times 350 \times 16/1000) + 0.92 \times (32 + 28)\} = 80 \text{ kN} < 1.5 V_{fl} = 1.5 \times 85 \approx 128 \text{ kN}$
translational stiffness of the ground storey (soft storey): $K_{eff} = \sum_{i=1}^n K_i \Delta\Phi_i^2 = K_1 \times 1^2 = K_1$	$K_{eff} = 4 \text{ (corner columns)} \times 3810 \text{ kN/m} + 4 \text{ (per. columns)} \times 4910 \text{ kN/m} + \text{(central column)} \times 3810 \text{ kN/m} \approx 38690 \text{ kN/m}$
FRP as shear reinforcement: For simplicity: $1.5V_{fl} = \max(1.5V_{fl,corner}, 1.5V_{fl,peripheral})$ $V_{Rd,o} = \min(V_{Rd,o,corner}, V_{Rd,o,peripheral})$ $V_{Rd,f} = 1.5V_{fl} - V_{Rd,o} = (2t_f/b) \times bh \times E_f \times \varepsilon_{fu,h}$	$1.5V_{fl} = \max(99 \text{ kN}, 128 \text{ kN}) \approx 128 \text{ kN}$ $V_{Rd,o} = \min(60 \text{ kN}, 80 \text{ kN}) = 60 \text{ kN}$ $\Delta V = 1.5V_{fl} - V_{Rd,o} = 68 \text{ kN}$ $\Delta V = V_{Rd,f} = (2t_f/b) \cdot bh \cdot E_f \cdot \varepsilon_{fu,h} \rightarrow$ $68,000 \text{ Nt} = (2t_f/250) \times 250 \times 350 \times 165,000 \times 0.0085 \rightarrow t_f = 0.07 \text{ mm} < t_o = 0.12 \text{ mm} \rightarrow 1 \text{ layer}$
Equation (10)	for $D_b = 14 \text{ mm}$, $\mu_{fr} = 1$, $N_b = 3$, $\varepsilon_{f,sl} = 0.0015$, $t_f = nt_o$, $A_{st} = 2 \times \pi \times 6^2/4 = 56.5 \text{ mm}^2$, $f_{y,st} = 240 \text{ MPa}$ and $s = 150 \text{ mm}$: $2.3 = (2 \times 1)/(3.14 \times 14)(0.33 \times 56.5 \times 240/(3 \times 150) + 2 \times t_f \times 165,000 \times 0.0015)/3 \rightarrow t_f = 0.25 = n \times 0.12 \rightarrow n = 2 \text{ layers}$
Equation (11b) Equation (11c) Equation (11a)	$\alpha_f = 1 - ((250 - 2.33)^2 + (350 - 2 \times 33)^2)/(3 \times 250 \times 350) = 0.56$ $\rho_{sv} = ((2 \times 200 + 2 \times 300) \times 28.26)/(150 \times 200 \times 300) = 0.00314$ $\varepsilon_{cu,c} = 0.005 = 0.0035 + 0.075[1(0.56 \times \rho_{fv} \times 165,000 \times 0.0085 + 0.15 \times 0.00314 \times 240)/16 - 0.1] \rightarrow \rho_{fv} = 0.0023$ and $\rho_{fv} = 2t_f(b+h)/(bh) \rightarrow$ $0.0023 = 2t_f(350+250)/(350 \times 250) \rightarrow t_f = 0.17 \text{ mm}$ $t_f = nt_o \rightarrow 0.17 \text{ mm} = n \times 0.12 \text{ mm} \rightarrow n = 2 \text{ FRP layers}$
Equation (12)	$\mu_\Delta = 1.3 + 12.4 \times (0.5 \times 0.56 \times 0.0033 \times 165000 \times 0.0085/16 - 0.1) = 1.06 \geq 1.3$ thus $\mu_\Delta = 1.3$

Table A1. Cont.

Formulae	Computation
<p>The load from the slabs is assumed to be transferred to beam B1. Conservatively, it is assumed that the loads transferred from the slab to B1 correspond to a quarter of the area of the slab. Hence, the total linear load for the seismic combination is:</p> $g = [((1/4 \times 6 \times 5 \times 0.2))6]_{\text{slab}} \times 25 + (0.2 \times 0.2)_{\text{beam}} \times 25 + [((1/4 \times 6 \times 5))6]_{\text{slab}} \times 2 = 9.75 \text{ kN/m,}$ $q = [((1/4 \times 6 \times 5))6]_{\text{slab}} \times 3.5 = 4.38 \text{ kN/m and } g + 0.3q = 9.75 + 0.3 \times 4.38 = 11.06 \text{ kN/m,}$ $(V_{g+\psi q,b})_l = (g + 0.3q)l/2 = (11.06 \times 6)/2 = 33.19 \text{ kN.}$ <p>Equation (13): $V_{j,v} = \Sigma M_{yc}(1/jd_c - 1/L_{b,n} \times H_n/H) + 1/2 (V_{g+\psi q,b})_l - (V_{g+\psi q,b})_r = 101 \times 10^3(1/((250 - 2 \cdot 30)) - 1/3000 \times 3000/2700) + 1/2 \times 33.19 - 0 = 510.8 \text{ kN}$</p>	
Equation (14)	$V_{j,h} = 134 \times 10^3(1/(0.9 \times 370) - 1/3000 \times 2500/2325) = 354.4 \text{ kN}$

References

- Fib Bulletin 14. *Externally Bonded FRP Reinforcement for r.c. Structures*; Report by Task Group 9.3; Fédération Internationale du Béton (fib): Lausanne, Switzerland, 2001; p. 130.
- Ruggieri, S.; Calo, M.; Cardellicchio, A.; Uva, G. Analytical-mechanical based framework for seismic overall fragility analysis of existing RC buildings in town compartments. *Bull. Earthq. Eng.* **2022**, *20*, 8179–8216. [\[CrossRef\]](#)
- Leggeri, V.; Ruggieri, S.; Zagari, G.; Uva, G. Appraising seismic vulnerability of masonry aggregates through an automated mechanical-typological approach. *Autom. Constr.* **2021**, *132*, 103972. [\[CrossRef\]](#)
- fib Bulletin 90. *Externally Applied FRP Reinforcement for Concrete Structures*; Technical Report, Task Group 5.1; Fédération Internationale du Béton (fib): Lausanne, Switzerland, 2019; ISBN 978-2-88394-131-1.
- Pantazopoulou, S.; Tastani, S.P.; Thermou, G.; Triantafillou, T.; Monti, G.; Bournas, D.; Guadagnini, M. Background to European seismic design provisions for the retrofit of R.C. elements using FRP materials. *Fib Struct. Concr.* **2015**, *17*, 194–219. [\[CrossRef\]](#)
- Bilotta, A.; Ceroni, F.; Di Ludovico, M.; Nigro, E.; Pecce, M.; Manfredi, G. Bond Efficiency of EBR and NSM FRP Systems for Strengthening Concrete Members. *ASCE J. Compos. Constr.* **2011**, *15*, 757–772. [\[CrossRef\]](#)
- Bournas, D.; Triantafillou, T. Flexural strengthening of reinforced concrete columns with near-surface-mounted FRP or stainless steel. *ACI Struct. J.* **2009**, *106*, 495–505.
- Coelho, M.; Sena-Cruz, J.; Neves, L. A review on the bond behavior of FRP NSM systems in concrete. *Constr. Build. Mater.* **2015**, *93*, 1157–1169. [\[CrossRef\]](#)
- Dias, S.; Barros, J. Shear strengthening of RC beams with NSM CFRP laminates: Experimental research and analytical formulation. *Compos. Struct.* **2013**, *99*, 477–490. [\[CrossRef\]](#)
- Novidis, D.; Pantazopoulou, S. Bond Tests of Short NSM—FRP & Steel Bar Anchorages. *ASCE J. Compos. Constr.* **2008**, *12*, 323–333.
- Sharaky, I.; Torres, L.; Baena, M.; Miàs, C. An experimental study of different factors affecting the bond of NSM FRP bars in concrete. *Compos. Struct.* **2013**, *99*, 350–365. [\[CrossRef\]](#)
- Thermou, G.; Pantazopoulou, S. Criteria and methods for redesign and retrofit of old structures. In Proceedings of the 10th U.S. National Conference on Earthquake Engineering, Frontiers of Earthquake Engineering, Anchorage, AK, USA, 21–25 July 2014.
- Pantazopoulou, S.; Guadagnini, M.; D'Antino, T.; Lignola, G.; Napoli, A.; Relafonzo, R.; Pellegrino, C.; Prota, A.; Balafas, I.; Tastani, S.; et al. Confinement of RC elements by means of EBR-FRP Systems, Chapter 5. In *Design Procedures for the Use of Composites in Strengthening of Reinforced Concrete Structures—State of the Art Report of RILEM TC 234-DUC*; Pellegrino, C., Sena-Cruz, J., Eds.; RILEM STAR Book Series; Springer: Berlin/Heidelberg, Germany, 2016. [\[CrossRef\]](#)
- Tastani, S.; Pantazopoulou, S.; Zdoumba, D.; Plakantaras, V.; Akritidis, E. Limitations of FRP jacketing in confining old-type reinforced concrete members in axial compression. *ASCE J. Compos. Constr.* **2006**, *10*, 13–25. [\[CrossRef\]](#)
- Pellegrino, C.; Modena, C. Analytical model for FRP confinement of concrete columns with and without internal steel reinforcement. *ASCE J. Compos. Constr.* **2010**, *14*, 693–705. [\[CrossRef\]](#)
- Biskinis, D.; Fardis, M. Models for FRP-wrapped rectangular RC Columns with Continuous or Lap-Spliced Bars under Cyclic Lateral Loading. *Eng. Struct.* **2013**, *57*, 199–212. [\[CrossRef\]](#)
- Tastani, S.; Balafas, I.; Dervis, A.; Pantazopoulou, S. Effect of Core Compaction on Deformation Capacity of FRP-Jacketed Concrete. *Constr. Build. Mater.* **2013**, *47*, 1078–1092. [\[CrossRef\]](#)
- Bousselham, A. State of Research on Seismic Retrofit of RC Beam-Column Joints with Externally Bonded FRP. *ASCE J. Compos. Constr.* **2010**, *14*, 49–61. [\[CrossRef\]](#)
- Akguzel, U.; Pampanin, S. Assessment and Design Procedure for the Seismic Retrofit of Reinforced Concrete Beam-Column Joints using FRP Composite Materials. *ASCE J. Compos. Constr.* **2012**, *16*, 21–34. [\[CrossRef\]](#)
- Del Vecchio, C.; Di Ludovico, M.; Balsamo, A.; Prota, A.; Manfredi, G.; Dolce, M. Experimental Investigation on Exterior RC Beam-Column Joints Retrofitted with FRP Systems. *ASCE J. Compos. Constr.* **2014**, *18*, 1–13. [\[CrossRef\]](#)
- Del Vecchio, C.; Di Ludovico, M.; Prota, A.; Manfredi, G. Analytical Model and Design Approach for FRP Strengthening of non-Conforming RC Corner Beam-Column Joints. *Eng. Struct.* **2015**, *87*, 8–20. [\[CrossRef\]](#)
- Frascadore, R.; Di Ludovico, M.; Prota, A.; Verderame, G.; Manfredi, G.; Dolce, M.; Cosenza, E. Local Strengthening of RC Structures as a Strategy for Seismic Risk Mitigation at Regional Scale. *Earthq. Spectra* **2015**, *31*, 1083–1102. [\[CrossRef\]](#)

23. Tureyen, A.; Frosch, R. Concrete Shear Strength: Another Perspective. *ACI Struct. J.* **2003**, *100*, 609–615.
24. Richart, F.; Brandtzaeg, A.; Brown, R. *Study of Failure of Concrete under Combined Compressive Stresses*; Engineering Experiment Station, No. 185; University of Illinois: Urbana, IL, USA, 1928.
25. Clough, R.; Penzien, J. *Dynamics of Structures*, 2nd ed.; McGraw-Hill International Editions: New York, NY, USA, 1993.
26. Rozman, M.; Fajfar, P. Seismic response of RC frame building designed according to old and modern practices. *Bull. Earthq. Eng.* **2009**, *7*, 779–799. [[CrossRef](#)]
27. Valente, M.; Milani, G. Alternative retrofitting strategies to prevent the failure of an under-designed reinforced concrete frame. *Eng. Fail. Anal.* **2018**, *89*, 271–285. [[CrossRef](#)]
28. *EN 1998-3 NEN SC8 PT3*; Eurocode 8—Design of Structures for Earthquake Resistance—Part 3: Assessment and Retrofitting of Buildings and Bridges. European Committee for Standardization (CEN): Brussels, Belgium, 2021.
29. *EN 13791*; Assessment of In-Situ Compressive Strength in Structures and Precast Concrete Components. European Committee for Standardization (CEN): Brussels, Belgium, 2019.
30. *ACI CODE-318-19*; Building Code Requirements for Structural Concrete and Commentary. American Concrete Institute: Farmington Hills, MI, USA, 2019.
31. Bentz, E.C. Sectional Analysis of Reinforced Concrete Members. Ph.D. Thesis, Department of Civil Engineering, University of Toronto, Toronto, ON, Canada, 2000; p. 184.
32. Thermou, G.E.; Pantazopoulou, S.J.; Elnashai, A.S. Global interventions for seismic upgrading of substandard rc buildings. *ASCE J. Struct. Eng.* **2012**, *138*, 387–401. [[CrossRef](#)]
33. *EN 1998-3*; Eurocode 8: Design of Structures for Earthquake Resistance—Part 3: Assessment and Retrofitting of Buildings. European Committee for Standardization (CEN): Brussels, Belgium, 2005.
34. Dai, K.Y.; Yu, X.H.; Lu, D.G. Phenomenological hysteretic model for corroded RC columns. *Eng. Struct.* **2020**, *210*, 110315. [[CrossRef](#)]
35. *EN 1998-1*; Eurocode 8: Design of Structures for Earthquake Resistance—Part 1: General Rules, Seismic Actions and Rules for Buildings. European Committee for Standardization (CEN): Brussels, Belgium, 2004.
36. Greek Seismic Assessment and Retrofit Code, Earthquake Planning and Protection Organization, 2017. Official Government Gazette 2984 B, 30-8-2017. Available online: www.oasp.gr (accessed on 11 December 2022).